Early indicators improve confidence in precipitation change and emergence

- 2 Megan Lickley^{1,2} and Sarah Fletcher^{3,4}
- ¹Earth Commons, Georgetown University, Washington DC, USA
- ²Science, Technology and International Affairs Program, School of Foreign Service, School of
- 5 Foreign Service, Georgetown University, Washington DC, USA
- ³Civil and Environmental Engineering, Stanford University, Stanford CA, USA
- ⁴Woods Institute for the Environment, Stanford University, Stanford CA, USA
- 9 Corresponding author: Megan Lickley (<u>megan.lickley@georgetown.edu</u>

10 **Key Points:**

8

11

12

13

- We develop a method to reduce uncertainty in precipitation change by integrating observations
- If precipitation will change, emergence will be sooner and more widespread than previous estimates
- In most regions, we expect to have advanced warning time of precipitation emergence

Abstract

17

36

- 18 Climate models disagree on the direction of precipitation change over ~40% of the Earth.
- 19 Current characterizations of expected change use the ensemble mean, which systematically
- 20 underestimates the magnitude and overestimates the time of emergence (ToE) of precipitation
- change in regions of high uncertainty. We develop a new approach to estimate both ToE and the
- 22 potential to update uncertainty in precipitation over time with new observations. Further, we
- 23 develop two new metrics that increase the usefulness of ToE for adaptation planning. The time of
- confidence (ToC) estimates when projections of precipitation emergence will have high
- confidence. Second, the advance warning time (AWT) indicates how long policymakers will
- 26 have to prepare for a new precipitation regime after they know change is likely to occur. Our
- 27 approach uses individual model projections that show change before averaging across models to
- calculate ToE. It then applies a Bayesian method to constrain uncertainty from climate model
- 29 ensembles using a perfect model approach. Results demonstrate the potential for widespread and
- decades-earlier precipitation emergence, with potential for end-of-century emergence to occur
- across 99% of the Earth compared to 60% in previous estimates. Our method reduces uncertainty
- in the direction of change across 8% of the globe. We find positive estimates of AWT across
- most of the Earth; however, in 30% of regions there is potential for no advanced warning before
- new precipitation regimes emerge. These estimates can guide adaptation planning, reducing the
- risk that policymakers are unprepared for precipitation changes that occur earlier than expected.

Plain Language Summary

- 37 Understanding if and when precipitation will change in response to anthropogenic warming is needed for
- 38 policymakers to design adaptation plans. However, climate model projections of precipitation are highly
- uncertain, with models disagreeing on the direction of change across 40% of Earth's surface. We develop
- a methodology for estimating when uncertainty will be resolved and estimating the emergence of new
- 41 precipitation regimes, demonstrating previous estimates projected change too late. We also estimate how
- 42 much advance warning time policymakers will have between learning that precipitation will change and
- 43 the onset of such change. We demonstrate that precipitation change is more widespread and sooner than
- 44 previously expected, but that most regions will have advance warning. Together, our findings provide
- 45 information that policymakers can use to more effectively adapt to climate change before impacts occur.

1 Introduction

- 47 Adapting to climate change requires knowledge of both *how* and *when* the climate will change.
- 48 General Circulation Models (GCMs) are the best tools for studying the evolution of future
- 49 anthropogenic climate change. However, GCM projections of many key societal impacts like
- 50 precipitation change exhibit large uncertainties. Indeed, across ~40% of Earth's surface, GCMs
- disagree on even the sign of precipitation change (see Figure 5a), with little progress in new
- 52 GCM generations (Knutti et al., 2013; Nguyen et al., 2018; Ukkola et al., 2020). This level of
- 53 uncertainty in GCM projections has made adaptation planning more challenging as planners are
- uncertain of whether a climate will get wetter or drier.
- 55

- The magnitude of precipitation change is commonly estimated using the multi-model mean
- 57 (MMM) of GCM ensembles along with a measure of model uncertainty, such as the fraction of
- models that agree in the direction of change (Kattsov et al., 2013; Knutti & Sedláček, 2012;
- Meehl, 2007; Lee et al., 2021). Likewise, the *timing* of the onset of a new climate regime, often
- 60 referred to as the Time of Emergence (ToE), is commonly estimated as the time when the MMM
- change exceeds some measure of background noise (Giorgi & Bi, 2009; King et al., 2015;
- Nguyen et al., 2018; Rojas et al., 2019). In regions of high uncertainty, averaging across GCM

projections with different directions of change systematically results in misleadingly low estimates in the expected magnitude of change. This approach also provides misleadingly late estimates of ToE, posing a risk that policymakers will be unprepared for new precipitation regimes that arise earlier than anticipated. This is an instance of Jensen's inequality (Jensen, 1906), popularized as the "flaw-of-averages" (Savage, 2002) and known to be an issue in many model-averaging applications (Cade, 2015). A few studies of ToE have addressed the flaw in averaging ensembles before calculating ToE, (King et al., 2015; Kusunoki et al., 2020; Mahlstein et al., 2012; Maraun, 2013), but still systematically underestimates ToE by including ensemble members that do not project emergence.

In addition to the bias embedded in current ToE estimates, ToE also has limited usefulness for adaptation planning in its current form. While characterizations of future climate change are typically focused on long-term change (mid- or end-of-century change; IPCC, 2021), regional adaptation decisions are made iteratively on shorter timescales. Therefore, reliable advanced warning of precipitation change a decade in advance can be more useful for adaptation planning than highly uncertain long-term projections (Herman et al., 2020). Current estimates of the magnitude of precipitation change and ToE provide static projections of expected long-term precipitation change and emergence; the literature does not indicate how quickly these expected values can change as new observations are collected. However, recent methods from Bayesian statistics have been developed to estimate how long-term projections of change can be informed from near-term observations. Mansfield et al. (2020), for example, use Gaussian process regression (GPR) trained on GCM output to predict long-term temperature change from shortterm observations. Integrating Bayesian models with GCM ensembles has been shown to reduce uncertainty in future precipitation projections (Fletcher et al., 2019; Smith et al., 2009; Tebaldi et al., 2004) and is capable of improving prediction accuracy (e.g., Massoud et al., 2020). While Bayesian methods have been applied to improve prediction of the magnitude and uncertainty of climate change, they have not addressed the time of emergence.

In this study, we develop a new approach to estimating the timing of precipitation change that: 1) addresses averaging bias, 2) updates estimates with new observations to reduce uncertainty, and 3) estimates the advance warning time of change for adaptation planning. We achieve this by developing a Bayesian framework applied to GCM ensembles for updating precipitation projections. Specifically, we use a GPR that exploits correlations between near-term and long-term precipitation change exhibited by GCMs (Figure S1c and d; Meehl, 2007; Watterson, 2008) to demonstrate how estimates of precipitation change can be updated over time as new observations are collected.

We apply our model to iteratively update the projected magnitude of precipitation change and estimate three new metrics. First, we estimate the *time of confidence* (ToC), the time when the future direction of precipitation change will be known with a high degree of confidence. We also re-evaluate ToE to correct averaging bias by estimating ToE conditional on emergence occurring; that is, using only GCM projections where emergence occurs (conditional ToE; ToE^C). This is analogous to standard methods for estimating daily precipitation probabilities by first estimating the probability of non-zero precipitation and then the magnitude of precipitation when it does occur (Waymire & Gupta, 1981). Finally, we introduce the *advance warning time* (AWT), which is the length of time before precipitation change emerges that policymakers will confidently know that change is coming and can prepare adaptation measures. Together, this approach improves estimates of the magnitude and timing of precipitation change both by

- realistically accounting for the full range of uncertainty in GCM ensembles today and also
- providing an approach to reduce uncertainty in the future as new observations become available.
- This allows us to provide insight on how far in advance planners can expect to have confidence
- about new precipitation regimes, developing more useful emergence metrics for adaptation
- planning.

2 Methods

- In the following, we present our modeling approach for estimating the time of confidence (ToC),
- the conditional time of emergence (ToE^C) and the lag time between these; the advanced warning
- time (AWT). First, we present the data used in our analysis. We then present our modeling
- framework for estimating our metrics of interest (ToC, ToE^C, and AWT) given a probabilistic
- Bayesian model. Finally, we present the details of the Bayesian model that updates predictions of
- precipitation change over time along with corresponding uncertainties using available
- observations.
- 124 *2.1 Data*
- 125 Analysis is conducted using a multi-model ensemble of 16 GCMs from Phase 5 of the Coupled
- Model Intercomparison Project (CMIP5). CMIP5 was published ~ 11 years prior to writing this
- manuscript which allows us to consider how a decade of new observations, that could not have
- been used to tune the GCMs, can be used to update the posteriors (described below). All GCMs
- are forced by the RCP 4.5 constant composition commitment scenario, where emissions follow
- the RCP 4.5 emissions pathway from 2005-2150, after which atmospheric concentrations of
- greenhouse gases are held constant at 2150 values. We use monthly precipitation output from
- 132 1850 2175 in our analysis. A list of GCMs used in the analysis is provided in Table S1.

133

- Observational data come from the CRU TS version 4.0 gridded data set (Harris et al., 2020),
- which provides monthly precipitation data over land from 1901-2020 at a 0.5° latitude x
- 136 0.5° longitude resolution.

137

- All data are spatially averaged at a 6°latitude x 6°longitude grid cell resolution. We conduct all
- analysis on standardized 5-year average increments of the log transform of annual precipitation,
- where data is standardized relative to the historical period; 1875-1950 for GCMs and 1901-1950
- for CRU. Results are retransformed and presented as percent change in precipitation. These
- spatial and temporal scales are chosen to be large enough to reduce noise but small enough to
- provide predictions on scales meaningful for decision makers, for example for river basin
- planning.

145 146

2.2 Modeling Framework

- Figure 1 illustrates our method for estimating our metrics of interest. We estimate these metrics
- by developing a Bayesian predictive model that quantifies the uncertainty in future precipitation
- change from GCM ensembles and updates uncertainty with data as new observations become
- available. To analyze how this may reduce uncertainty in the future, we use synthetic data.
- Specifically, we use a perfect model experiment approach, where one GCM at a time is left out
- of the ensemble (henceforth referred to as out-of-sample GCM (OOS GCM)). The OOS GCM is
- treated as the true climate trajectory which we 'observe' over time, and the remaining GCMs are
- treated as the ensemble used to develop the Bayesian model's prior mean and covariance
- function. The predictive model then iteratively predicts future precipitation change (along with
- uncertainties of future change) as larger portions of the OOS GCM are 'observed'. This allows

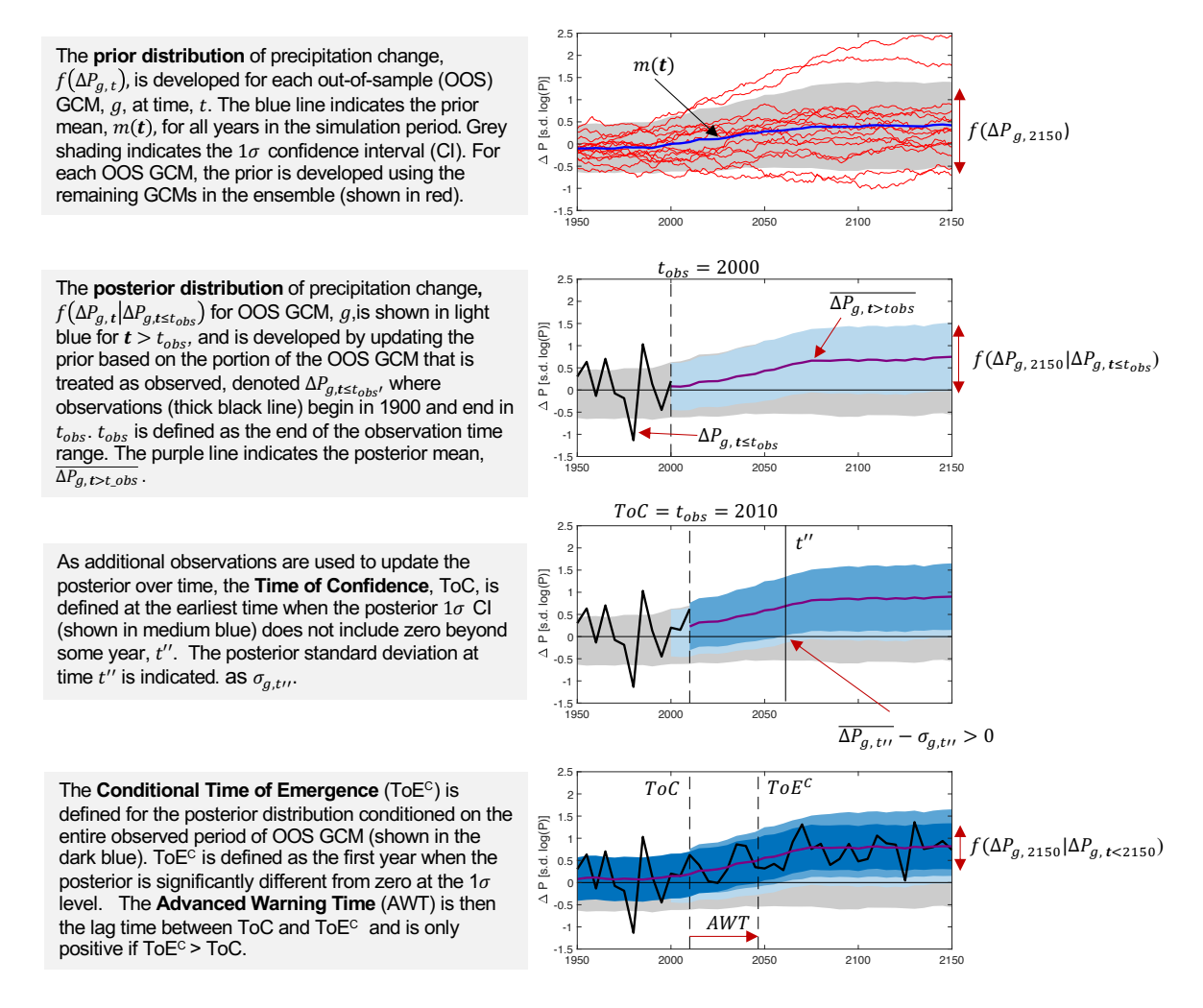


Figure 1: Modeling framework illustrating how the Time of Confidence, conditional Time of Emergence, and Advanced Warning Time are estimated for one out-of-sample (OOS) GCM using the predictive model. This is then repeated such that each GCM is treated as an OOS GCM once in each grid cell to provide an ensemble of posterior distributions and metrics.

Updating uncertainty in precipitation projections using OOS GCMs To estimate metrics for each OOS GCM, g, the timeseries is divided into two periods; the first period starting in 1875 until time t_{obs} , is treated as the historical period when precipitation observations are made, henceforth referred to as OOS virtual observations. The second period, from t_{obs} to 2150 is treated as the future that we seek to project (Figure 1). This allows us to project a probability distribution of future precipitation in time t given historical OOS virtual

- observations $f(\Delta P_{g,t}|\Delta P_{g,t\leq t_{obs}})$. For each OOS GCM, we iteratively update the posterior over 174
- time with more OOS virtual observations, first using $t_{obs} = 1975$ and then sequentially extending 175
- the historical period by 5-year increments up until 2150. We extract the posterior mean, 176
- $\overline{\Delta P_{g,t}}$, and standard deviation $\sigma_{g,t}$ and use them to estimate when the precipitation will be 177
- significantly different than historical. Specifically, we define precipitation change to be 178
- significant for time t when the 1-sigma confidence interval $(\overline{\Delta P_{a,t}} \sigma_{a,t}, \overline{\Delta P_{a,t}} + \sigma_{a,t})$ does not 179
- contain zero. For each grid cell, this provides us with 16 OOS GCMs, and thus 16 projections of 180
- how uncertainty is updated over time, and 16 projections of when precipitation change is 181
- 182 significant.
- 183
- 184 Updating uncertainty in precipitation projections using CRU data
- Using OOS GCMs to update uncertainty, as described above, allows us to simulate how 185
- uncertainty may evolve in the future as new observations are collected. Additionally, we can 186
- assess how uncertainty has changed to date using real observational data that has become 187
- available since CMIP5 was published. Analogous to the OOS GCM, we apply GPR to CRU 188
- observations by using the GCM ensemble to develop a probability distribution of future 189
- precipitation projections given CRU observations: $f(\Delta P_t | \Delta P_{CRU})$. We then repeat the estimation 190
- 191 of whether precipitation change is significant as in the previous section.
- 192 Defining ToC, ToE and AWT
- Using these precipitation projections updated over time, we next develop three new temporal 193
- metrics that estimate: when we will have confidence about the direction of precipitation change, 194
- when precipitation will enter a new climate regime, and how far in advance we will know the 195
- 196 new regime is coming. First, the Time of Confidence (ToC), characterizes the time when we are
- confident that future precipitation will be significantly different from historical climatology. 197
- 198 Second, if the future will be significantly different, what year will that difference be detectable?
- We define this time as the conditional Time of Emergence (ToE^C) where "conditional" indicates 199
- 200 that it is estimated only for GCM realizations when future change occurs. This is in contrast to
- ToE^{MMM}, which refers to the definition often seen in the literature, defined when the MMM 201
- exceeds some level of background noise (Giorgi & Bi, 2009). Third, the Advanced Warning 202
- Time (AWT) is the length of lead time between learning that precipitation will change and the 203
- onset of such change, estimated as ToE^C ToC. AWT thus indicates the amount of time planners 204
- will have to implement adaptation measures appropriate for the direction of precipitation change. 205
- To estimate ToC, we iteratively update the posterior 1- σ CI ($\overline{\Delta P_{g,t}} \sigma_{g,t}$, $\overline{\Delta P_{g,t}} + \sigma_{g,t}$) for all 206
- $t \in T$ as t_{obs} is extended forward. We define t'' as the first year when the posterior CI doesn't 207
- contain zero i.e. the first year precipitation change is significant. We define $ToC_g = t_{obs}$ for the 208
- earliest t_{obs} when this condition holds (See Figure 1). That is, ToC_q , is the time at which we 209
- know, at the 1- σ level confidence, that precipitation at some time in the future will be 210
- significantly different from historical climatology. There are instances when only a portion of 211
- the posterior CIs from t'' to 2150 remains significantly different from zero: we only define ToC_a 212
- if at least half of the years beyond t'' are also significantly different from zero. 213
- To estimate ToE^C, we assume full knowledge of the OOS GCM time series, comparable to 214
- previous methods for estimating ToE (Giorgi & Bi, 2009; Mahlstein et al., 2012). We define 215
- ToE_g^C as the first year, t'' when the posterior CI doesn't contain zero where the posterior is updated using *all* OOS virtual observations from 1875 2150. It is customary in the literature to 216
- 217

extend ToE analysis out to 2100 and if ToE does not occur by 2100, to characterize it as not emerging. Ending our analysis in 2100 does not meaningfully alter our findings.

219 220 221

222

223

218

Finally, we define AWT for each GCM g, as: $AWT_g = ToE_g^C - ToC_g$. If AWT is positive, then ToE_g^c occurred after ToC_{g_i} was defined (see Figure 1), indicating there was advanced warning of change. If AWT is negative, then $ToE_{g_i}^C$ occurs first and ToC_{g_i} is only established in hindsight. In these instances, we are only confident in the direction of change after the signal has emerged.

224 225

Aggregating across OOS GCM projections 226 To estimate each of our metrics (ToC, ToE^C and AWT), we first estimate each metric separately 227 for each GCM in each grid cell as described above. We then define expected values within each 228 229 grid cell by averaging over GCMs, resulting in expected values of ToC, ToE^C and AWT. Importantly, we only include OOS GCMs that have a defined significant emergence before the 230 end of our analysis in 2150 in our average. In addition to calculating averages, we also count the 231 number of OOS GCMs that have a defined significant emergence. Additionally, we calculate 232 averages over three subsets of GCMs: those exhibiting significant drying (G_D) , significant 233 wetting (G_W) , or significant change in either direction of change $(G_{D \cup W})$. For example, 234 $E[ToC_{G_D}]$ denotes the expected value of ToC for a drier future, which is estimated as the mean 235 ToC value for the subset of OOS GCMs that project a drier future. This can be interpreted as: if 236 the future will be drier, when can we expect to know?

237

238

239

240

241

242

243

244

245

246 247

248

249

250

251

2.3 Predictive Model: Gaussian Process Regression

To estimate the probabilities of future precipitation change defined in the previous section, we develop a predictive model that exploits temporal correlations in GCM projections using a Gaussian process regression (GPR) (Rasmussen & Williams, 2006). GPR is a non-parametric Bayesian machine learning technique that estimates a posterior distribution updated with observations, either from historical data or synthetic data from the OOS GCMs. The model is developed by specifying a prior using a Gaussian process with mean m, and covariance defined by a kernel function, K. m and K are functions of an input vector t, which here refers to a vector of 5-year increments from 1875-2150, our study period. The mean, m(t), then defines a time series of prior expected precipitation values and the kernel K describes the similarity between precipitation values based on how close they are in time. Additionally, we define $t \le t_{obs}$ as a vector of 5-year increments from 1875 to t_{obs} , the historical period for which observations are available. $\Delta P_{g,t \le t_{obs}}$ is the vector of precipitation observations during the historical period $t \le t_{obs}$ from OOS GCM g, and $\Delta P_{g,t}$ is the vector of precipitation we are estimating across the full study period t.

252 253

254

$$\begin{bmatrix} \Delta P_{g,t \le t_{obs}} \\ \Delta P_{g,t} \end{bmatrix} = \mathcal{N} \begin{pmatrix} m(\mathbf{t} \le t_{obs}), \begin{bmatrix} K(\mathbf{t} \le t_{obs}, \mathbf{t} \le t_{obs}) + \sigma_n^2 I & K(\mathbf{t} \le t_{obs}, \mathbf{t}) \\ K(\mathbf{t}, \mathbf{t} \le t_{obs}) & K(\mathbf{t}, \mathbf{t}) \end{bmatrix} \end{pmatrix},$$

255 256

where σ_n^2 represents the variance of the standardized residuals of the observations. $\overline{\Delta P_{q,t}}$ is the mean of the posterior distribution, which is estimated as:

257 258

$$\overline{\Delta P_{g,t}} = m(t) + K(t, t \le t_{obs}) (K(t \le t_{obs}, t \le t_{obs}) + \sigma_n^2 I)^{-1} (\Delta P_{t \le t_{obs}} - m(T_{t \le t_{obs}})),$$

259 260 261

Similarly, we define $cov(\Delta P_{a,t})$ as the covariance of the posterior distribution, estimated as:

 $cov\big(\Delta P_{a,t}\big) = K(\boldsymbol{t},\boldsymbol{t}) - K(\boldsymbol{t},\boldsymbol{t} \leq t_{obs})(K(\boldsymbol{t} \leq t_{obs},\boldsymbol{t} \leq t_{obs}) + \sigma_n^2 I)^{-1} K(\boldsymbol{t} \leq t_{obs},\boldsymbol{t}).$

These posterior mean estimates, along with their covariance, provide us with the posterior probability distribution of the underlying mean change in precipitation at any time t: $f(\Delta P_{g,t}|\Delta P_{g,t\leq t_{obs}})$. This is then used to estimate ToC, ToE and AWT, as described above. We use $\sigma_{g,t}$ to denote the standard deviation of $cov(\Delta P_{g,t})$ going forward.

Further details regarding model parameterization are found in the SI (Text S1).

Predictive Model Validation

273 Finally, we validate the model by testing how well the posterior distribution,

 $f(\Delta P_{g,t>t_{obs}} | \Delta P_{g,t\leq t_{obs}})$, predicts OOS GCM precipitation values after t_{obs} given values of t_{obs} 274 equal to 2000, 2020, 2040, 2060 and 2080. We find good model agreement: on average between 275 68 and 70% of $\Delta P_{g,t>t_obs}$ values (across all grid cells and all OOS GCMs) fall within the 68% 276 posterior CI, and between 93.5 and 94.7% of $\Delta P_{g,t>t_{obs}}$ values fall within the 95% posterior CI. 277 There is some spatial variability to accuracy with polar regions performing slightly better (94-278 279 96% accuracy) compared to the tropics (92-93% accuracy). In addition, using the entire GCM simulation period, we find that at the 95% CI, the model is able to accurately predict long-term 280 (i.e. 23rd century) direction of change with an 81% accuracy by 2020 and an 85% accuracy by 281 2050. This validates that the Bayesian model is in-fact narrowing in on the "true" OOS future 282

3 Results

climate trajectory.

262

263 264

265

266

267 268 269

270 271

272

283 284

285

286

287

288

289

290 291

292 293

294

295

296

297

298

299

300

301

302

303

304

305

306

Updating uncertainty in precipitation projections with new observations

Our modeling results indicate that we can expect substantial near-term uncertainty reductions in long-term precipitation projections (Figure 2). We include illustrations of uncertainty reductions over time when precipitation projections are constrained by OOS virtual observations (Figure 2 subplots).

First, we consider when at least half of the OOS GCMs are confident that 2100 precipitation will be significantly different at the 1-sigma confidence level (see Methods). For the prior distribution, we find that only 36% of grid cells (weighted by area) meet the 1-sigma significance criteria for at least half of OOS GCMs (Figure 2 maps). This means that in 64% of grid cells, the majority of the OOS GCM prior 1-sigma CIs of 2100 precipitation change contain zero and are therefore not significant. In approximately half of these grid cells (31% of global surface area), the majority of OOS GCM projections do not emerge by 2100. However, in $\sim 1/4$ (2/3^{rds}) of the remaining grid cells (equivalent to 8% (20%) of global surface area), the posterior $\overline{\Delta P_{g,2100}}$ CIs are significant for more than half of OOS GCMs for $t_{obs} = 2020$ ($t_{obs} = 2060$). The reduction of this uncertainty across OOS GCMs for these select time periods is indicated by stippling color in Figure 2's map. This uncertainty reduction is expected to occur in both wet and dry regions of high uncertainty, and in particular over land in the lower latitudes. This underscores that although GCMs disagree on future precipitation trends across 64% of the planet, by integrating OOS observations up to 2020 (2060) we can expect to have confidence in the direction of 2100 precipitation change in ~13% (31%) of this area.

Figure 2 subplots illustrate how uncertainty reductions can lead to emerging trends in locations where the prior range encompasses zero (e.g. Syria). They also show how uncertainty in the precipitation trend is reduced over time, which can inform us that long-term change may be insignificant (Kenya), or more extreme than the prior range (Greenland). This indicates that near-term observations are highly valuable in constraining long-term change, thus providing useful insights for adaptation planning.

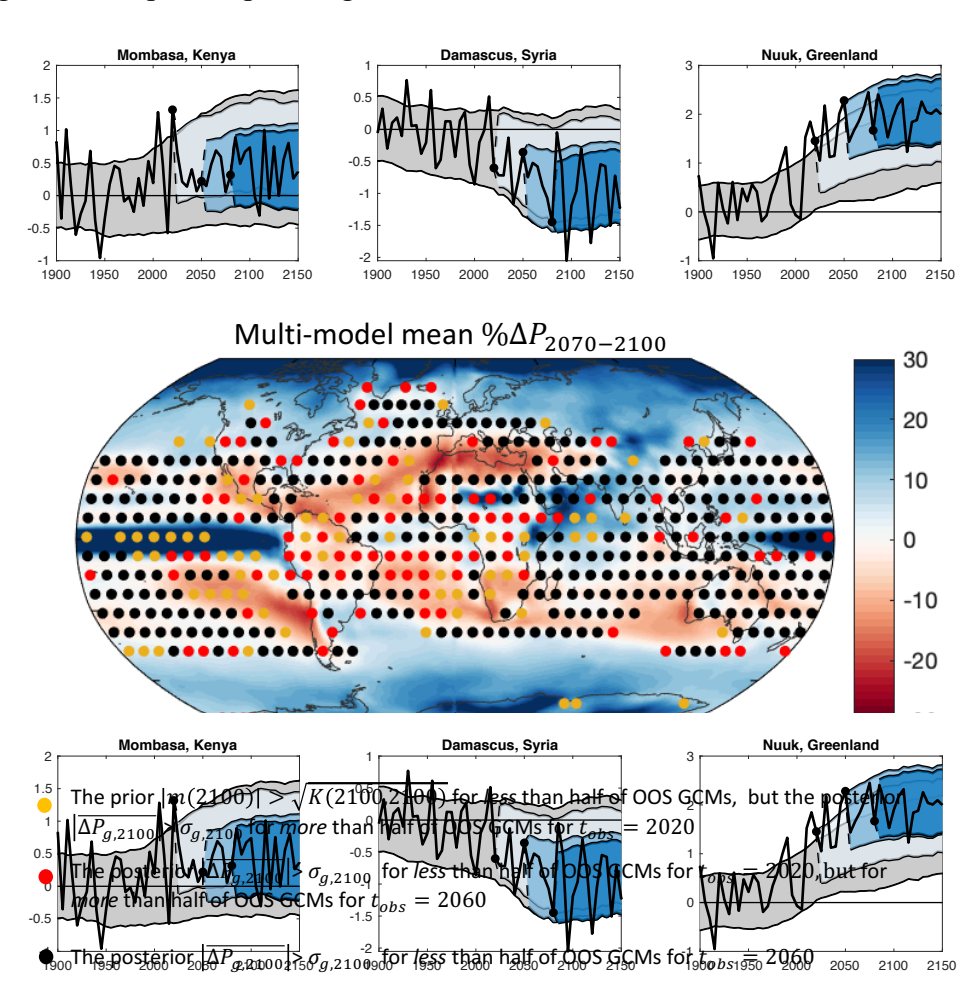


Figure 2: Global map of the multi-model mean percentage change in annual precipitation in 2070 – 2100 relative to 1900 – 1950; subplots illustrate uncertainty updating over time for one OOS GCM example (bcc-csm1; see methods). There is no stippling if the prior mean magnitude of 2100 precipitation change exceeds 1σ for at least half of the OOS GCMs. Otherwise, yellow (red) stippling indicates that the posterior mean magnitude of 2100 precipitation change exceeds 1σ when t_{obs} is equal to 2020 (2060) for at least half of the OOS GCMs. Black stippling indicates that fewer than half of OOS GCMs posterior means 2100 change exceed 1σ in 2060 (i.e. when $t_{obs} = 2060$). Subplots illustrate the evolution of $f(\Delta P_{g,t>t_{obs}}|\Delta P_{g,t\leq t_{obs}})$ for one possible OOS GCM trajectory in sample grid cells at a 6°x6° resolution. Y-axes corresponds to precipitation change in units of standard deviations in log (*P*) relative to historical mean log(*P*). Black lines show precipitation trajectories at 5-year averages for the OOS GCM. Grey shading indicates the prior 1σ confidence interval for $f(\Delta P_{g,t})$. Dots indicate the last year of OOS data, t_{obs} , used in

updating posterior distribution, $f(\Delta P_{g,t>t_{obs}}|\Delta P_{g,t\leq t_{obs}})$, for three time periods; $t_{obs}=2020$ (light blue), $t_{obs}=2050$ (medium) blue, and $t_{obs}=2080$ (dark blue). Shading indicates a 1σ (68%) confidence interval.

Global Estimates of ToE, ToC, and AWT

Figure 2 aggregates across all OOS GCM members, including members that do not emerge. We next consider the time of confidence for only the OOS GCMs that do exhibit emergence. Figure 3 illustrates our global estimates of expected ToE^C , ToC, and AWT. Early ToC occurs in regions of high certainty in future change, whereas late ToCs occur in regions where the MMM signal is small relative to the noise ratio; ToC and the MMM signal to noise ratio are strongly negatively correlated (with Spearman's rank correlation of $\rho = -0.85$, p-value <<0.01). Of particular note, our model suggests that ToC is expected to have been defined by 2020 over most land regions, with the exception of Australia. This suggests that if we constrain GCM projections with historical observational data in our Bayesian framework, there is potential to have confidence the future will be wetter or drier in most land regions.

Expected ToE^C is shown in the second row of Figure 3, illustrating both earlier and more widespread expected ToE^C values relative to ToE^{MMM} estimates (for comparison see Figure 5b; Giorgi & Bi, (2009)). Regions where models tend to agree on long-term change (e.g. polar regions) also have early expected ToE^C values. Regions that, according to GCMs, could get wetter but it is unlikely, coincide with late ToE^C_{GW} estimates (e.g. southeastern US and northern Africa; Figure 3d). These expected ToE^C estimates indicate that there is potential for widespread emergence, globally, throughout this century (Figure 3f). This is in contrast to ToE^{MMM} estimates (Giorgi & Bi, 2009; Figure 5b) where emergence is constrained to regions with strong agreement across GCMs. However, similar to ToE^{MMM} , expected ToE^C also correlates strongly with the MMM signal to noise ratio (with Spearman's rank correlation of $\rho = -0.68$, p-value << 0.01), thus providing similar spatial patterns of relative emergence to earlier methods, while emerging much earlier on average. This is quantified further in Figure 4.

The third row of Figure 3 shows the expected AWT conditional on future change. Green regions delineate regions where AWT is positive, indicating advance warning of future change and brown colors delineate regions where AWT is negative, indicating that ToC occurs only in hindsight after ToE^{C} has occurred. Negative AWT values are widespread in regions where there is potential for future change of opposite sign to the GPR prior. For example, in regions where the prior indicates a future more likely to be wet, a longer duration of a drying trend is required before we have confidence that the future is in fact drying, and not simply exhibiting an anomalous drought. In these instances, ToE^{C} has already occurred before we have confidence that the trend will continue. Because most global surface area is projected to be wetter, negative AWT values are more wide spread for drier futures. AWT patterns thus exhibit similarities with the MMM magnitude and uncertainty in GCM projections (Figure 5a) and are positively correlated with the MMM signal to noise ratio (with Spearman's rank correlation of $\rho=0.45$, p-value <<0.01).

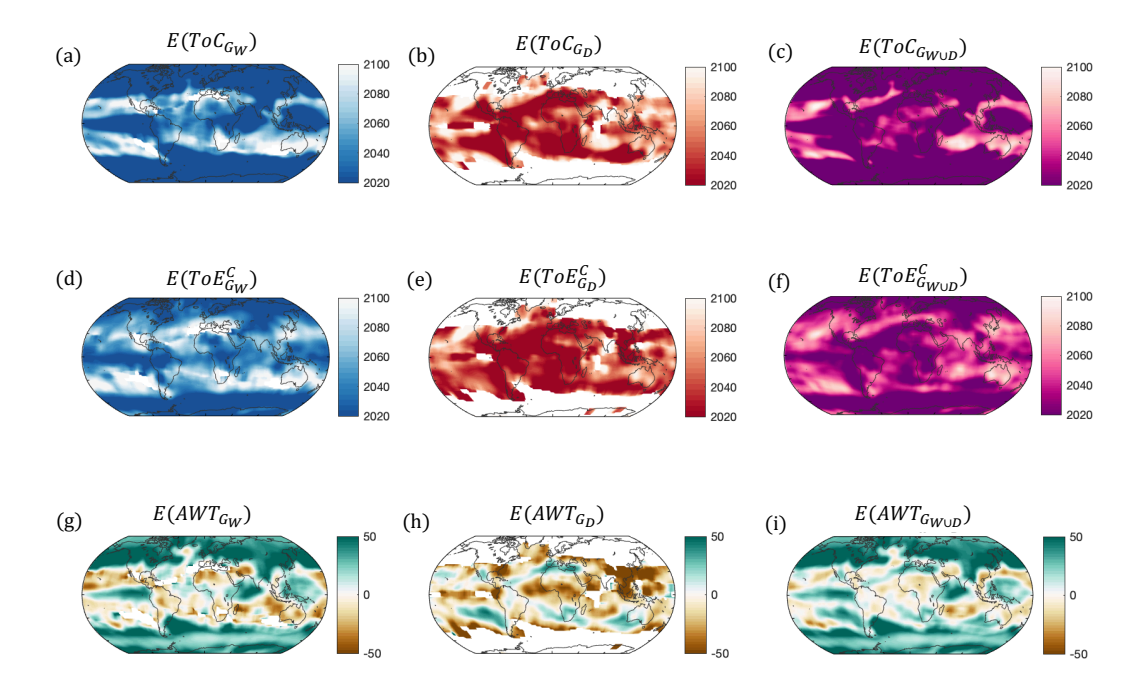


Figure 3: Spatial patterns of expected time of confidence (ToC), conditional time of emergence (ToE^C), and advanced warning time (AWT). (a) The CMIP5 multi-model expected ToC in which we learn that the future will be wetter at the 1σ confidence level. (b) as in (a) but for a future that is drier. (c) as in (a) but for the future that is either wetter or drier. (d) The expected time of emergence conditioned on the future GCM projection being wetter at the 1σ confidence level. (e) as in (d) but for a drier future. (f) as in (d) but for a future that is either wetter or drier. (g) Expected AWT for a wetter future (i.e. (d) minus (a)). (h) as in (g) but for a drier future. (i) as in (g) but for a future that is either wetter or drier. For (a) - (i), values are estimated at the 6° latitude x 6° longitude grid cell level and smoothed using a moving 10° x 10° degree moving window. The colors are saturated at 2020 and 2100. These years were chosen so as to illustrate locations where we should have sufficient observations to be able to detect ToC at the time of writing this paper, and also to focus on what we can learn over the course of the 21^{st} century. Locations that are white occur where the metric is never defined.

Figure 4(a – c) compares the cumulative emergence of expected ToE^C to that of ToE^{MMM} at both the 1- σ and 2- σ level. This shows that by 2050, ToE^C is expected to have occurred over 75% of Earth's surface area at the 1σ level, much higher than the 40% estimate from the ToE^{MMM} approach (Figure 5c). To be clear, this indicates that over 75% of global surface area, it is expected that if emergence occurs, it will do so prior to 2050. This difference in extent of precipitation emergence between ToE estimation methods remains pronounced throughout the century, such that by 2100 there is potential for ToE^C to be defined over 99% of Earth's surface area, compared to 57% from the ToE^{MMM} approach. The contrast between ToE methods is most pronounced in regions that could dry, where ToE^C_{GD} is expected to have occurred over 41% of Earth's surface area by 2050, but ToE^{MMM} estimates only 9% of surface area to have dry emergence by 2050. This suggests the need for greater urgency in adaptation planning in the agriculture and water sectors in many water-stressed regions than previously anticipated.

Figure 4 (d – f) shows the cumulative areal extent of expected ToC in regions that could become wetter, drier, or both. Our GPR approach suggests that by 2020 (2050), expected ToC will be defined over as much as 57% (78%) of global surface area (Figure 4 f). Note that expected ToC only encompasses OOS GCMs that exhibit emergence. This therefore indicates that across 57% (78%) of global surface area, if mean precipitation is changing, we can expect to be confident by 2020 (2050) in the direction of this change. In the remaining 43% (22%) of surface area, we expect to still be uncertain about the direction of future precipitation change in these years.

Figure 4 (g – i) shows the cumulative distribution of AWT for regions with a future that could be significantly wetter, drier, or both. For regions that could be wetter in the future (over as much as ~87% of global surface area at the 1σ level), the majority of regions (~60% of global surface area) have a positive AWT with about 25% of global surface area seeing the potential to have negative AWT for wet regions. The remaining 2% of surface area reflects the potential error where ToC is defined in instances that do not emerge. The majority of regions that could be drier, however, are expected to have a negative AWT (~34% of global surface area at the 1σ level), compared to 20% of global surface area where a positive AWT of a dry future is expected. This again underscores the challenges that planners face for preparing for water stress, as most regions are not expected to have advance warning of new, drier climates before they occur.

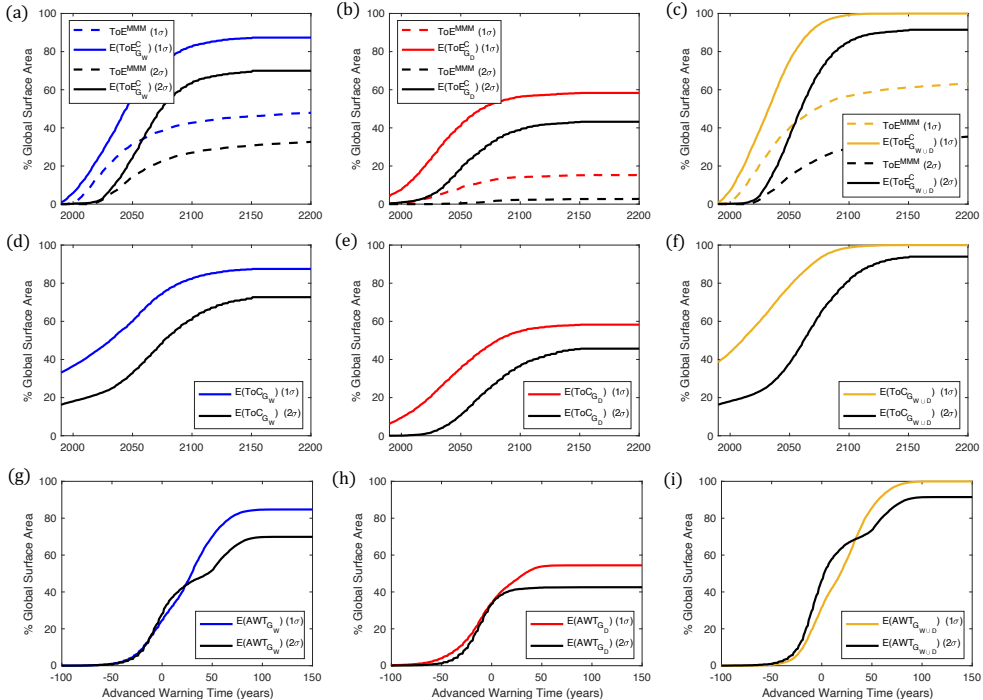


Figure 4. Expected time of emergence (ToE), time of confidence (ToC), and advanced warning time (AWT) conditioned on future change. (a) – (c) Cumulative percentage of global surface area where expected ToE^C ($E(ToE^C)$), is defined conditional on change (solid lines), compared to ToE^{MMM} estimates (dashed lines). Colored (black) indicate when $E(ToE^C)$, is defined at the 1σ (2σ) confidence level. (a) Shows the percent of global surface area where $E(ToE_{G_W}^C)$, indicates a wetter future. (b) as in (a) but for a drier future. (c) as in (a) but for either wetter or drier future. (d) – (f) as in (a) – (c) but for the expected time of confidence (ToC). (g) – (i) as in

(a) – (c) but for the expected advanced warning time. Negative values indicate the fraction of global surface area where ToE^{C} occurs before ToC.

Expected change and ToE estimates based on historical data

Finally, we evaluate expected changes in precipitation and expected ToE given available observations over land and compare this with MMM estimates. In this analysis, we use historical precipitation data instead of OOS GCMs as the observations in the Bayesian model, reflecting the best available information to date rather than potential future observations. Figure 5 provides an update of expected future precipitation change $f(\Delta P_{2085}|\Delta P_{CRU,t\leq 2020})$, and ToE estimates, $E(ToE_{CRU})$ given observed precipitation from CRU TS data available from 1900 – 2020 (Harris et al., 2020). Note that this is different than ToE^C since we are not estimating ToE conditional on future change, however, it is an improvement from ToE^{MMM} as it constrains future projections of change using available observations. For our Bayesian estimated precipitation change, we select the year 2085 as it is the mid-point over the MMM averaged time period and thus provides a more direct comparison across methods.

Both the MMM and Bayesian modeling approach result in similar patterns of expected precipitation change given CRU observations. For the Bayesian model, we note less uncertainty over land and more pronounced drying in mid-latitudes relative to the MMM approach (Figure 5(a) and (c)). According to our model and observations, $E(ToE_{CRU}^{C})$ has occurred prior to 2020 over most of the land area North of 30°N along with some regions in Northern Africa, which have been drying, and parts of southern South America. While much of the uncertainty shown in Figure 5(c) coincides with regions of late ToC shown in Figure 5(c), one exception is over much of Africa. This suggests that either emergence will not occur over much of Africa or that data and/or GCM projections are insufficiently accurate to provide reliable indicators of change. This calls for improved data collection and modeling efforts over Africa, as many populations in this continent are highly vulnerable to precipitation change (Niang et al., 2015) and thus require the best information for adaptive responses to climate change.

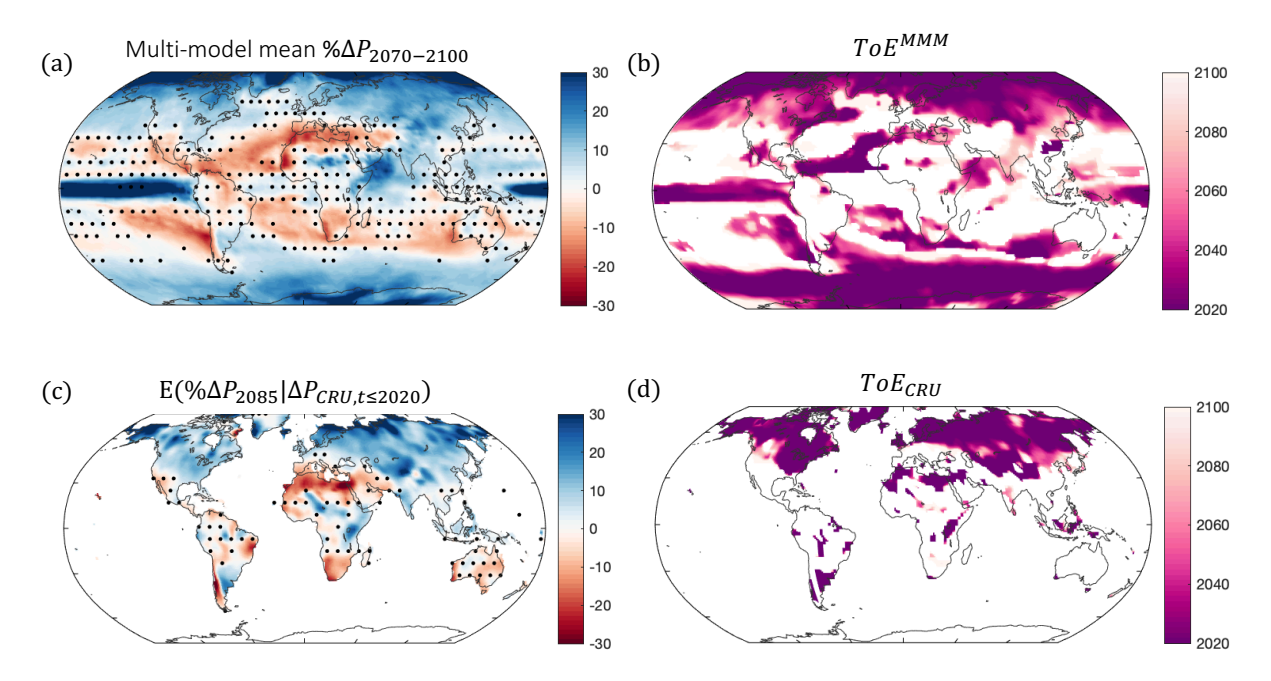


Figure 5. Standard versus Bayesian modeled expected change and time of emergence (ToE). (a) CMIP5 multi-model mean (MMM) projected percent change in precipitation ($\%\Delta P$) in 2070-2100 relative to 1900-1950. Grey areas indicate where change is within 5% of historical values. Stippling indicates where fewer than 70% of models agree on the direction of change. (b) Time of Emergence of precipitation signal following Giorgi and Bi (2009), where the signal is the MMM 30-year moving average and the noise is the square root of the MMM historical decadal variance. Values prior to 2000 and after 2100 are saturated. White indicates regions where the signal never exceeds the noise throughout the simulation period. (c) Bayesian expected change in precipitation in 2085 relative to 1901-1950 values, conditioned on CRU observational precipitation data available from 1901 – 2020 (Harris et al., 2020). Stippling indicates where the probability of change in less than 70%. (d) Expected ToE conditioned on CRU observations (E(ToE_{CRU})). White indicates where data is missing over the oceans, or where expected emergence over land is not projected to occur given available observations.

4. Discussion

Averaging across uncertain GCM ensembles has led to a literature that systematically underestimates the magnitude of potential precipitation change and overestimates the amount of uncertainty. This has led to a further systematic overestimation of the time of emergence of the anthropogenic signal (e.g. see Stocker et al., 2013 and references therein). Further, the common characterization of static uncertainty in climate science has challenged the development of adaptation approaches that respond to evolving uncertainty. While the adaptation literature has widely adopted adaptive management approaches, most of those approaches underestimate the value of adaptive management by not explicitly quantifying opportunities to reduce uncertainty in the future (Fletcher et al., 2019). To our knowledge, the present manuscript provides the first framework to globally quantify the potential for present *and* future uncertainty reductions in a Bayesian modeling framework. This is achieved by treating OOS GCMs as potential future observations in our Bayesian model, illustrating how future projections of precipitation change

and uncertainty will be updated if the OOS GCM trajectory is observed. In doing so we can 485 iteratively update uncertainty distributions and re-evaluate the significance of the climate signal. 486 As such, this is the first study to develop a framework that estimates the time in which we will be 487 able to confidently predict that the future will be significantly wetter or drier than historical 488 values (ToC). Our analysis shows that according to GCM projections, presently there has been 489 sufficient anthropogenic change to define ToC over most surface area (Figure 3c) and reduce the 490 uncertainty in the direction of change across 8% of global surface area (Figure 2) at a 1-sigma 491 confidence level, which equates to a 13% reduction in the areal extent of uncertainty in the 492 direction of precipitation change. 493

494 495

496

497

- This methodology was tested on annual mean precipitation for emissions scenario (RCP 4.5) and at one spatial scale (6° latitude x 6° longitude). In line with the Time of Emergence literature on precipitation change, we expect that ToC and ToE would be sensitive to seasonal choices, choice of extremes, spatial scale of interest, and the emissions trajectory (Gaetani et al., 2020; Maraun, 2013; Nguyen et al., 2018; Rojas et al., 2019).
- We apply our methodology to address the MMM flaw in estimating the time of emergence (ToE) 500 by both calculating ToE on individual GCMs rather than the MMM and only estimating ToE 501 conditional on future emergence occurring. As such, we identify widespread potential for ToE^C 502 onset. We show that if emergence does occur it will be substantially earlier than the literature 503 currently predicted (Giorgi & Bi, 2009; Mahlstein et al., 2012). We find that 75% of the Earth's 504 surface may see emergence of new precipitation regimes by 2050, which is 90% higher than 505 estimated extent of emergence at that time from Giorgi & Bi (2009). Our estimates of ToE^C are 506 earlier than TOEMMM over 88% of global surface area, with a mean ToE^C of 2043 across 507 locations where TOEMMM predicts no emergence. These findings indicate a broad need to 508 consider earlier adoption of adaptation measures globally. 509
- An additional advantage of our approach to calculating ToE is that we use a novel Bayesian modeling framework to constrain estimates of ToE from GCMs using observations of precipitation change. While common ensemble approaches indicate that GCMs either project no change or are uncertain about future change across ~40% of global surface area (Figure 5a) and
- across 45% of global land area. We find there is potential to reduce this uncertainty to 29% of global surface area (a 35% reduction in areal extent of uncertainty over land) using historical
- precipitation data from CRU as observations in a Bayesian model to improve projections. This
- 517 highlights the value of integrating physical models of the climate system with data-driven
- methods using hybrid approaches in improving projections of climate change impacts (e.g.
- Lickley et al., 2020, 2021). Patterns of early expected ToE, conditional on CRU observations are
- largely consistent with observed signal to noise ratios of mean precipitation change (Hawkins et
- 521 al., 2020).
- Finally, the lag time between learning with confidence that future change will occur (ToC) and
- 523 the emergence of such change (ToE) provides the advanced warning time (AWT) for planners.
- We find that over most global surface area, there is positive AWT (Figure 3i and Figure 4i),
- especially in regions with high agreement across GCMs in projections of significant change, with
- an average of 38 years (26 years) of advance warning at the 1- σ level (2- σ level). This provides
- an estimate of how much time policymakers will have to plan adaptations in advance of knowing adaptations are needed. However, we find negative AWT estimates over ~30% of global surface
- area, concentrated in locations with a low but non-zero chance of drying. In these areas,

- policymakers face "deep" uncertainty (Walker et al., 2013), necessitating more challenging and
- costly adaptation strategies that will be robust to a wide range of future climate conditions.
- 532 **Data and Code.**
- All code will be made available through a published github repository prior to publication. All
- GCM data used in this work are available at https://esgf-node.llnl.gov/projects/cmip5/.
- Observational data comes from Harris et al. (2020) and is available at
- 536 <u>https://crudata.uea.ac.uk/cru/data/hrg/.</u>
- Acknowledgements. We thank Daniel Gilford, Ben Santer, Noah Diffenbaugh, Amanda Giang,
- Morgan Edwards, and Claudia Tebaldi for helpful conversations. This material is based upon
- work supported by the National Science Foundation under Grant 2207036.

References

541

- Cade, B. S. (2015). Model averaging and muddled multimodel inferences. *Ecology*, *96*(9), 2370–2382. https://doi.org/10.1890/14-1639.1
- Fletcher, S., Lickley, M., & Strzepek, K. (2019). Learning about climate change uncertainty enables flexible water infrastructure planning. *Nature Communications*, 10(1), 1–11. https://doi.org/10.1038/s41467-019-09677-x
- Gaetani, M., Janicot, S., Vrac, M., Famien, A. M., & Sultan, B. (2020). Robust assessment of the time of emergence of precipitation change in West Africa. *Scientific Reports*, 10(1), 1–10. https://doi.org/10.1038/s41598-020-63782-2
- Giorgi, F., & Bi, X. (2009). Time of emergence (TOE) of GHG-forced precipitation change hotspots. *Geophysical Research Letters*, *36*(6), 1–6. https://doi.org/10.1029/2009GL037593
- Harris, I., Osborn, T. J., Jones, P., & Lister, D. (2020). Version 4 of the CRU TS monthly highresolution gridded multivariate climate dataset. *Scientific Data*, 7(1), 1–18. https://doi.org/10.1038/s41597-020-0453-3
- Hawkins, E., Frame, D., Harrington, L., Joshi, M., King, A., Rojas, M., & Sutton, R. (2020).
 Observed Emergence of the Climate Change Signal: From the Familiar to the Unknown.
 Geophysical Research Letters, 47(6). https://doi.org/10.1029/2019GL086259
- Hay, C. C., Morrow, E., Kopp, R. E., & Mitrovica, J. X. (2014). Probabilistic reanalysis of
 twentieth-century sea-level rise. *Nature*, 517(7535), 481–484.
 https://doi.org/10.1038/nature14093
- Herman, J. D., Quinn, J. D., Steinschneider, S., Giuliani, M., & Fletcher, S. (2020). Climate
 Adaptation as a Control Problem: Review and Perspectives on Dynamic Water Resources
 Planning Under Uncertainty. *Water Resources Research*, 56(2).
 https://doi.org/10.1029/2019WR025502
- IPCC. (2021). Summary for Policymakers. In: Climate Change 2021: The Physical Science
 Basis. Contribution of Working Group I to the Sixth Assessment Report of the
 Intergovernmental Panel on Climate Change.
- Jensen, J. L. W. V. (1906). Sur les fonctions convexes et les inégalités entre les valeurs moyennes. *Acta Mathematica*, 30(1), 175–193. https://doi.org/10.1007/BF02418571
- Kattsov, V., Federation, R., Reason, C., Africa, S., Uk, A. A., Uk, T. A., et al. (2013). Evaluation of climate models. *Climate Change 2013 the Physical Science Basis: Working Group I*
- Contribution to the Fifth Assessment Report of the Intergovernmental Panel on Climate
- 574 *Change*, 9781107057, 741–866. https://doi.org/10.1017/CBO9781107415324.020

- King, A. D., Donat, M. G., Fischer, E. M., Hawkins, E., Alexander, L. V., Karoly, D. J., et al. (2015). The timing of anthropogenic emergence in simulated climate extremes. *Environmental Research Letters*, 10(9). https://doi.org/10.1088/1748-9326/10/9/094015
- Knutti, R., & Sedláček, J. (2012). Robustness and uncertainties in the new CMIP5 climate model
- projections. *Nature Climate Change*, 3(October), 1–5. https://doi.org/10.1038/nclimate1716 Knutti, R., Masson, D., & Gettelman, A. (2013). Climate model genealogy: Generation CMIP5
- and how we got there. *Geophysical Research Letters*, *40*(6), 1194–1199. https://doi.org/10.1002/grl.50256

- Kusunoki, S., Ose, T., & Hosaka, M. (2020). Emergence of unprecedented climate change in projected future precipitation. *Scientific Reports*, 10(1), 1–8. https://doi.org/10.1038/s41598-020-61792-8
- Lee, J.-Y., Marotzke, J., Bala, G., Cao, L., Corti, S., Dunne, J. P., et al. (2021). 2021: Future
 Global Climate: Scenario-Based Projections and Near-Term Information. In M.-D. V., P.
 Zhai, A. Pirani, S. L. Connors, C. Péan, S. Berger, et al. (Eds.), Climate Change 2021: The
 Physical Science Basis. Contribution of Working Group I to the Sixth Assessment Report of
 the Intergovernmental Panel on Climate Change (pp. 553–672). Cambridge, United
 Kingdom and New York, NY, USA: Cambridge University Press.
 https://doi.org/10.1017/9781009157896.006
- Lickley, M., Solomon, S., Fletcher, S., Rigby, M., Velders, G. J. M., Daniel, J., et al. (2020).

 Quantifying contributions of chlorofluorocarbon banks to emissions and impacts on the
 ozone layer and climate. *Nature Communications*, *11*(1380).

 https://doi.org/10.1038/s41467-020-15162-7
- Lickley, M., Fletcher, S., Rigby, M., & Solomon, S. (2021). Joint Inference of CFC lifetimes and banks suggests previously unidentified emissions. *Nature Communications*, *12*(2920), 1–10. https://doi.org/https://doi.org/10.1038/s41467-021-23229-2 |
- Mahlstein, I., Portmann, R. W., Daniel, J. S., Solomon, S., & Knutti, R. (2012). Perceptible changes in regional precipitation in a future climate. *Geophysical Research Letters*, 39(5), 1–5. https://doi.org/10.1029/2011GL050738
- Mansfield, L. A., Nowack, P. J., Kasoar, M., Everitt, R. G., Collins, W. J., & Voulgarakis, A. (2020). Predicting global patterns of long-term climate change from short-term simulations using machine learning. *Npj Climate and Atmospheric Science*, *3*(1). https://doi.org/10.1038/s41612-020-00148-5
 - Maraun, D. (2013). When will trends in European mean and heavy daily precipitation emerge? *Environmental Research Letters*, 8(1). https://doi.org/10.1088/1748-9326/8/1/014004
- Massoud, E. C., Lee, H., Gibson, P. B., Loikith, P., & Waliser, D. E. (2020). Bayesian model averaging of climate model projections constrained by precipitation observations over the contiguous United States. *Journal of Hydrometeorology*, *21*(10), 2401–2418. https://doi.org/10.1175/JHM-D-19-0258.1
- Meehl, G. A. (2007). Global Climate Projections. In S. Solomon (Ed.), *Climate Change 2007: The Physical Science Basis* (pp. 747–845). Cambridge, UK and New York: Cambridge
 Univer Press.
- Nguyen, T. H., Min, S. K., Paik, S., & Lee, D. (2018). Time of emergence in regional precipitation changes: an updated assessment using the CMIP5 multi-model ensemble. *Climate Dynamics*, *51*(9–10), 3179–3193. https://doi.org/10.1007/s00382-018-4073-y
- Niang, I., Ruppel, O. C., Abdrabo, M. A., Essel, A., Lennard, C., Padgham, J., & Urquhart, P. (2015). Africa. *Climate Change 2014: Impacts, Adaptation and Vulnerability: Part B:*
- Regional Aspects: Working Group II Contribution to the Fifth Assessment Report of the Intergovernmental Panel on Climate Change, 1199–1266.

https://doi.org/10.1017/CBO9781107415386.002

637

638

639

644

645

646

647

648

649

- Rasmussen, C. E., & Williams, C. K. I. (2006). *Gaussian Processes for Machine Learning*. Cambridge, Massachusetts: The MIT Press.
- Rojas, M., Lambert, F., Ramirez-Villegas, J., & Challinor, A. J. (2019). Emergence of robust precipitation changes across crop production areas in the 21st century. *Proceedings of the National Academy of Sciences of the United States of America*, 116(14), 6673–6678. https://doi.org/10.1073/pnas.1811463116
- Savage, S. (2002). Forum The Flaw of Averages by. *Harvard Business Review*, 80(11), 20–21.
- Smith, R. L., Tebaldi, C., Nychka, D., & Mearns, L. O. (2009). Bayesian modeling of uncertainty in ensembles of climate models. *Journal of the American Statistical Association*, 104(485), 97–116. https://doi.org/10.1198/jasa.2009.0007
- Stocker, T. F., Qin, D., Plattner, G.-K., Tignor, M., Allen, S. K., Boschung, J., et al. (2013).

 Climate Change 2013: The Physical Science Basis. Contribution of Working Group I to the
 Fifth Assessment Report of the Intergovernmental Panel on Climate Change.
 - Tebaldi, C., Mearns, L. O., Nychka, D., & Smith, R. L. (2004). Regional probabilities of precipitation change: A Bayesian analysis of multimodel simulations. *Geophysical Research Letters*, *31*(24), 1–5. https://doi.org/10.1029/2004GL021276
- Ukkola, A. M., De Kauwe, M. G., Roderick, M. L., Abramowitz, G., & Pitman, A. J. (2020).
 Robust Future Changes in Meteorological Drought in CMIP6 Projections Despite
 Uncertainty in Precipitation. *Geophysical Research Letters*, 47(11), 1–9.
 https://doi.org/10.1029/2020GL087820
 - Walker, W. E., Haasnoot, M., & Kwakkel, J. H. (2013). Adapt or perish: A review of planning approaches for adaptation under deep uncertainty. *Sustainability (Switzerland)*, *5*(3), 955–979. https://doi.org/10.3390/su5030955
 - Watterson, I. G. (2008). Calculation of probability density functions for temperature and precipitation change under global warming. *Journal of Geophysical Research Atmospheres*, 113(12), 1–13. https://doi.org/10.1029/2007JD009254
- Waymire, E., & Gupta, V. (1981). A Mathematical Structure of Rainfall Representations 1. A
 Review of the Stochastic Rainfall Models. *Water Resources Research*, 17(5), 1261–1272.
 https://doi.org/10.1029/WR017i005p01261